THE JOURNAL OF BIOLOGICAL CHEMISTRY Vol. 272, No. 15, Issue of April 11, pp. 9922–9932, 1997
Printed in U.S.A.

The Nitric Oxide/Superoxide Assay

INSIGHTS INTO THE BIOLOGICAL CHEMISTRY OF THE NO/O_2^- INTERACTION*

(Received for publication, October 16, 1996, and in revised form, February 3, 1997)

Malte Kelm‡, Rüdiger Dahmann‡, David Wink§, and Martin Feelisch‡¶

From the ‡Department of Medicine, Division of Cardiology, Pulmonary Diseases, and Angiology, Heinrich Heine University, Moorenstrasse 5, D-40225 Düsseldorf, Federal Republic of Germany, and the §Tumor Biology Section, Radiation Biology Branch, NCI, National Institutes of Health, Bethesda, Maryland 20892-1002

Nitric oxide (NO) is a widespread signaling molecule involved in the regulation of an impressive spectrum of diverse cellular functions. Superoxide anions (O_2^-) not only contribute to the localization of NO action by rapid inactivation, but also give rise to the formation of the potentially toxic species peroxynitrite ($ONOO^-$) and other reactive nitrogen oxide species. The chemistry and biological effect of $ONOO^-$ depend on the relative rates of formation of NO and O_2^-. However, the simultaneous quantification of NO and O_2^- has not been achieved yet due to their high rate of interaction, which is almost diffusion-controlled. A sensitive spectrophotometric assay was developed for the simultaneous quantification of NO and O_2^- in aqueous solution that is based on the NO-induced oxidation of oxyhemoglobin (oxyHb) to methemoglobin and the O_2^--mediated reduction of ferricytochrome *c*. Using a photodiode array photometer, spectral changes of either reaction were analyzed, and appropriate wavelengths were identified for the simultaneous monitoring of absorbance changes of the individual reactions. oxyHb oxidation was followed at 541.2 nm (isosbestic wavelength for the conversion of ferri- to ferrocytochrome *c*), and ferricytochrome *c* reduction was followed at 465 nm (wavelength at which absorbance changes during oxyHb to methemoglobin conversion were negligible), using 525 nm as the isosbestic point for both reactions. At final concentrations of 20 μM ferricytochrome *c* and 5 μM oxyHb, the molar extinction coefficients were determined to be $\epsilon_{465-525}$ = 7.3 mM^{-1} cm^{-1} and $\epsilon_{541.2-525}$ = 6.6 mM^{-1} cm^{-1}, respectively. The rates of formation of either NO or O_2^- determined with the combined assay were virtually identical to those measured with the classical oxyhemoglobin and cytochrome *c* assays, respectively. The assay was successfully adapted to either kinetic or end point determination in a cuvette or continuous on-line measurement of both radicals in a flow-through system. Maximal assay sensitivity was ~25 nM for NO and O_2^-. Cross-reactivity with $ONOO^-$ was controlled for by the presence of L-methionine. Generation of NO from the NO donor spermine diazeniumdiolate could be reliably quantified in the presence and absence of low, equimolar, and high flux rates of O_2^-. Likewise, O_2^- enzymatically generated from hypoxanthine/xanthine oxidase could be specifically quantified with no difference in absolute rates in the presence or absence of concomitant NO generation at different flux rates. Nonenzymatic decomposition of 3-morpholinosydnonimine hydrochloride (100 μM) in phosphate buffer, pH 7.4 (37 °C), was found to be associated with almost stoichiometric production of NO and O_2^- (1.24 μM NO/min and 1.12 μM O_2^-/min). Assay selectivity and applicability to biological systems were demonstrated in cultured endothelial cells and isolated aortic tissue using calcium ionophore and NADH for stimulation of NO and O_2^- formation, respectively. Based on these data, a computer model was elaborated that successfully predicts the reaction of NO and O_2^- with hemoprotein and may thus help to further elucidate these reactions. In conclusion, the nitric oxide/superoxide assay allows the specific, sensitive, and simultaneous detection of NO and O_2^-. The simulation model developed also allows the reliable prediction of the reaction between NO and O_2^- as well as their kinetic interaction with other biomolecules. These new analytical tools will help to gain further insight into the physiological and pathophysiological significance of the formation of these radicals in cell homeostasis.

Nitric oxide (NO) is a widespread intracellular and intercellular signaling molecule involved in the regulation of diverse physiological and pathophysiological mechanisms in the cardiovascular system and the central and peripheral nervous systems and in immunological reactions (for review, see Refs. 1–3). In contrast to the current view that NO is extremely unstable *in vivo*, but in agreement with its functioning as a paracrine mediator, NO can travel significant distances to reach target cells neighboring the NO-generating cell (4, 5). Along this migration, in particular at higher concentration, NO can interact with molecular oxygen to form higher nitrogen oxides (*e.g.* NO_2 and N_2O_3), which can either react with other biomolecules such as thiols and amines or simply hydrolyze to form nitrite (NO_2^-) and nitrate (NO_3^-). Furthermore, NO rapidly reacts with reduced hemoproteins and oxygen-derived radicals. The extent of either of these reactions largely depends on the microenvironmental conditions under which NO is released, most important, the concentration of other bioreactants (6, 7).

There is increasing evidence that the effective concentration of NO in a given biological tissue is not solely determined by its rate of enzymatic formation, but also by its rate of degradation and scavenging by other biomolecules. For example, the progression of atherosclerotic lesions has been attributed to an increased oxidative stress within the vascular wall and, consequently, to an accelerated breakdown of NO (8, 9). One important oxygen-derived metabolite capable of inactivating NO is superoxide (O_2^-), which reacts with NO at an almost diffusion-controlled rate (10) to form peroxynitrite ($ONOO^-$) (Equation 1).

* This work was supported in part by Gerhard-Hess-Award Program Grant Ke 405/3 from the Deutsche Forschungsgemeinschaft. The costs of publication of this article were defrayed in part by the payment of page charges. This article must therefore be hereby marked "*advertisement*" in accordance with 18 U.S.C. Section 1734 solely to indicate this fact.

¶ To whom correspondence should be addressed. Tel. and Fax: 49-211-8118323; E-mail: Feelisch@aol.com.

$$NO + O_2^- \rightarrow ONOO^- \quad \text{(Eq. 1)}$$

Peroxynitrite can isomerize, via its conjugated acid, to nitrate, which has little biological activity in its own right (Equation 2).

$$ONOO^- + H^+ \rightleftharpoons ONOOH \rightarrow HNO_3 \rightleftharpoons H^+ + NO_3^- \quad \text{(Eq. 2)}$$

However, $ONOO^-$ itself forms a strong oxidant of potential pathophysiological significance that can react with a vast number of other biomolecules and can cause cell damage (11, 12). Furthermore, $ONOO^-$ can react with the remaining NO to form nitrogen dioxide (NO_2), which leads to the formation of the nitrosating agent N_2O_3 (13) (Equations 3 and 4).

$$ONOO^- + NO \rightarrow NO_2 + NO_2^- \quad \text{(Eq. 3)}$$

$$NO_2 + NO \rightleftharpoons N_2O_3 \quad \text{(Eq. 4)}$$

A variety of analytical techniques have been described for the quantification of either NO or O_2^-, some of which have been successfully applied to estimate the production of either radical in biological systems (for review, see Refs. 14–16). In contrast, only little is known about the formation of $ONOO^-$ in tissues and cells, and to the best of our knowledge, to date only qualitative data based on the detection of nonspecific secondary reaction products are available. Furthermore, under conditions where both NO and O_2^- are formed, almost all methods for measurement of either molecule can detect only that amount of radical that escaped from chemical interaction with the respective other reaction partner (and, of course, other biomolecules), leading to significant underestimation of their true rates of formation. To better understand the individual reactivity of NO and O_2^- in a biological system and to appreciate the pathophysiological consequences of their interaction, reliable information on individual flux rates is required.

The simultaneous monitoring of NO and O_2^-, although highly desirable, was believed to be technically unfeasible due to the extremely rapid reaction between both radicals. We describe here an analytical technique that allows, for the first time, the simultaneous and sensitive quantification of both NO and O_2^- and, under certain conditions, additionally helps to unmask the proportion of peroxynitrite and other reactive nitrogen oxide species formed. The results obtained with this new assay could be successfully simulated by a computer model that predicts the reaction of both radicals with hemoproteins and thus may give valuable new insights into the reaction between NO and O_2^- in biological systems.

EXPERIMENTAL PROCEDURES

Classical Oxyhemoglobin and Cytochrome c Assays—One of the few spectrophotometric techniques that allows the quantification of NO in aerobic aqueous solutions (the oxyhemoglobin assay) is based on the stoichiometric conversion by NO of oxyhemoglobin (oxyHb[1]; Fe^{2+}) to methemoglobin (metHb; Fe^{3+}) (17) (Equation 5).

$$\text{oxyHb} + NO \rightarrow \text{metHb} + NO_3^- \quad \text{(Eq. 5)}$$

The formation of NO can be continuously monitored by time-dependent recording of the absorbance changes in the Soret band associated with oxyHb oxidation. Maximal sensitivity is achieved by choosing a wavelength at which the extinction difference between oxyHb and metHb is maximal (*e.g.* 401 nm) and an isosbestic point (*e.g.* 411 nm) as an internal reference (dual-wavelength measurement) (Fig. 1*A*).

One of the most commonly used spectrophotometric assays for the quantification of O_2^- is based on the rapid reduction by O_2^- of ferricytochrome *c* (Fe^{3+}) to ferrocytochrome *c* (Fe^{2+}) (Equation 6),

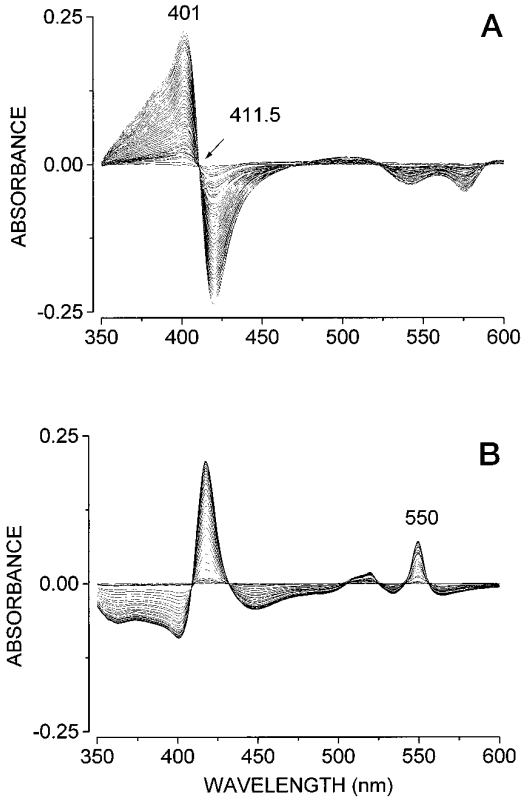

FIG. 1. **Representative difference spectral scans of the redox conversion of oxyHb to metHb and of ferricytochrome c to ferrocytochrome *c*.** *A*, the gradual oxidation of oxyHb (5 μM) to metHb was achieved by generation of NO from spermine NONOate (40 μM). *411.5* nm is the isosbestic point used mostly as an internal reference in the classical oxyHb assay, and *401* nm represents one of the wavelengths at which the absorbance difference between the oxidized and reduced forms of hemoglobin is maximal. *B*, the reduction of ferricytochrome *c* (5 μM) to ferrocytochrome *c* by O_2^- was enzymatically generated using xanthine oxidase and hypoxanthine (0.75 unit/ml and 25 μM, respectively). *550* nm denotes the monitoring wavelength used in the classical cytochrome *c* assay. Repeated scans were performed at 10-s intervals.

$$\text{Ferricytochrome } c\,(Fe^{3+}) + O_2^- \rightarrow \text{ferrocytochrome } c\,(Fe^{2+}) + O_2 \quad \text{(Eq. 6)}$$

which can be followed by monitoring the increase in absorbance at 550 nm (Fig. 1*B*) (18). Separate measurements of either NO or O_2^- formation for validation of the nitric oxide/superoxide assay were carried out in 100 mM phosphate buffer, pH 7.40 (37.0 ± 0.05 °C), using a conventional dual-wavelength double-beam spectrophotometer (UV-3000, Shimadzu, Duisburg, FRG) set to the classical detection wavelengths of the oxyHb and cytochrome *c* assays, respectively.

Combined Nitric Oxide/Superoxide Assay—The photometric assay for the simultaneous determination of NO and O_2^- described in this paper is based on a combination of the above-mentioned detection principles: the NO-mediated oxidation of oxyHb and the O_2^--induced reduction of ferricytochrome *c*. For the separate recording of either signal, a programmable diode array spectrophotometer (DU-7500i, Beckman, Munich, FRG) was used. In contrast to classical dual-wavelength spectrophotometers, the diode array technique has the advantage of allowing parallel monitoring of multiple wavelengths almost at the same time (*e.g.* an entire absorption spectrum can be derived within 0.1 s). As the internal memory of these machines is usually limited in capacity to the storage of a couple of full spectra or a few hundred data points only, a series of programs were developed for the continuous visualization of a large number of data points on the photometer screen and for the on-line transfer of raw data between photometer and personal computer to allow unlimited data sampling and post-processing of photometric recordings. Measurements were performed as either end point or kinetic determinations using glass or disposable plastic cuvettes or under conditions of continuous flow using a flow-through

[1] The abbreviations used are: oxyHb, oxyhemoglobin; metHb, methemoglobin; NDNDate, diazeniumdiolate; SIN-1, 3-morpholinosydnonimine hydrochloride; ECs, endothelial cells.

cuvette with a total volume of 80 μl (QS 178-010, Hellma, Mühlheim, FRG). If not otherwise indicated, all measurements were carried out in 100 mM phosphate buffer, pH 7.4, at 37 ± 0.02 °C using a thermostatted cuvette holder connected to a D 8-L water bath (Haake, Karlsruhe, FRG).

Adaptation to Diode Array Technique and Determination of Molar Extinction Coefficients—Consecutive spectral scans between 350 and 600 nm were recorded on oxidation of oxyHb to metHb using either aqueous solutions of authentic NO or spermine NONOate as NO donor. Changes in absolute spectra obtained with the diode array technique were virtually identical to those observed using a conventional dual-wavelength spectrophotometer (17). Difference spectra were derived by subtraction of individual spectral scans from the spectrum obtained with pure oxyHb at time 0 ($t_{0\ min}$). Increasing concentrations of oxyHb (0.1–7.0 μM) were reacted with excess NO or SIN-1, and the difference in absorbance between 401 and 411.5 nm (isosbestic point for oxyHb to metHb conversion) was recorded. Photometric readings were converted to NO concentrations using a molar extinction coefficient of $\epsilon_{401-411.5}$ = 49.5 $mM^{-1}\ cm^{-1}$ as determined under the conditions of this study. Reproducibility for end point determinations (repeated measurements of NO standards) was better than 4% (coefficient of variance = 3.4; n = 12). The molar extinction coefficient for the cytochrome c assay (ϵ_{550} = 19.5 $mM^{-1}\ cm^{-1}$) was determined by reacting increasing concentrations (5–30 μM) of ferricytochrome c with a 3-fold molar excess of ascorbic acid or the O_2^--generating hypoxanthine/xanthine oxidase system (n = 3 each) and recording changes in absorbance at 550 nm. The extinction coefficients for the NO-induced conversion of oxyHb to metHb ($\epsilon_{525-541.2}$) and for the O_2^--mediated conversion of ferri- to ferrocytochrome c ($\epsilon_{465-525}$) in the combined nitric oxide/superoxide assay were determined basically in the same manner, but in the presence of the respective other hemoprotein. Determinations were performed under conditions identical to those of the kinetic investigations. In those experiments where O_2^- was enzymatically generated using the hypoxanthine/xanthine oxidase system, the buffer was additionally supplemented with 25 μM EDTA.

Materials and Solutions—All compounds used in this study were either analytical grade or otherwise of the highest purity available. ABTS (2,2′-azinobis(3-ethylbenzthiazoline-6-sulfonic acid, diammonium salt), catalase (from bovine liver, thymol-free; 20,000 units/mg), 18-crown-6 (1,4,7,10,13,16-hexaoxacyclooctadecane), ferricytochrome c (from horse heart, containing 2% ferrocytochrome c and 2.7% water), hemoglobin (human, lyophilized), hypoxanthine, manganese dioxide (MnO_2; activated), L-methionine, potassium superoxide (KO_2), and superoxide dismutase (from bovine erythrocytes; 4400 units/mg of protein) were purchased from Sigma (Deisenhofen, FRG). Xanthine oxidase (from bovine milk, phosphate-free lyophilisate; 0.18 unit/mg) was obtained from Boehringer (Mannheim, FRG). Sodium nitrite ($NaNO_2$), hydrogen peroxide (H_2O_2; 30%), and pyrogallol (1,2,3-trihydroxybenzene) were from Merck (Darmstadt, FRG). Spermine NONOate (Cayman Chemical Co., Inc., Ann Arbor, MI) was dissolved in argon-gassed 0.01 M NaOH. SIN-1 (kindly donated by Dr. K. Schönafinger, Hoechst Marion Roussel, Frankfurt/Main, FRG) was dissolved in distilled water adjusted to pH 5.0. *S*-Nitrosoglutathione was synthesized according to Hart (19) and dissolved in de-aerated citrate buffer, pH 2.0. NO donor stock solutions were kept on ice in the dark for up to 3 h. Aqueous solutions of authentic NO were prepared essentially as described (20). Briefly, argon (quality = 5.0, >99.99% argon; Linde AG, Unterschleissheim, FRG) was passed through a closed all-glass system comprising two scrubbing bottles, one containing an alkaline pyrogallol (5%, w/v) solution for removal of traces of oxygen and the other containing potassium hydroxide (10%, w/v) to scavenge higher oxides of nitrogen, connected in series with a three-necked beaker containing saline (0.9% NaCl) for the dissolution of NO. After flushing with argon for 30 min, the gas flow was switched to NO (quality = 3.0, >99.9% NO; AGA GAS GmbH, Hamburg, FRG) and maintained for a further 45 min. Aliquots were transferred to air-tight syringes via a septum with the system kept under positive pressure with NO to avoid changes in NO concentration due to re-equilibration between the aqueous and gas phases. Concentrations ranged between 1.7 and 2 mM NO, depending on the ambient pressure and temperature. Dilutions were made in deoxygenated and argon-flushed saline, and concentrations were determined immediately before application using the gas-phase chemiluminescence reaction with ozone (21). Stock solutions of O_2^- (0.1–10 mM) were prepared by dissolving solid KO_2 in water-free dimethyl sulfoxide containing 0.5% crown ether (22). Aqueous stock solutions of $ONOO^-$ were prepared by mixing $NaNO_2$ and H_2O_2 in a quenched-flow reactor as described (12). Peroxide contamination after treatment with MnO_2 was typically below 0.05% as assessed using the horseradish peroxidase-catalyzed ABTS cation radical formation as described (23). Frozen aliquots (final concentration = 250–350 mM) were stored at −80 °C for up to 4 weeks with only minor decomposition. Dilutions were made in 0.01 M NaOH and used immediately. Decomposed $ONOO^-$ was prepared by dilution of the stock solution in 1 M hydrochloric acid and readjustment with NaOH to pH 13 after 5 min. Oxyhemoglobin was prepared as described in detail elsewhere (17). Aliquots of the stock solution (1.9–2.5 mM, expressed as concentration in heme) were stored at −80 °C for up to 6 months. Ferricytochrome c was used without further purification.

Biological Sources of NO and O_2^-—Endothelial cells (ECs) were harvested enzymatically from porcine aorta using collagenase and cultured in M199 medium (Boehringer Mannheim) containing 20% newborn calf serum. Antibiotics were omitted from the medium from day 5 after isolation. The cells were passaged twice using trypsin/EDTA, grown to confluence on plastic dishes (Primaria, Falcon, Heidelberg, FRG), and characterized morphologically by their typical cobblestone-like growth pattern as well as by uptake of acetylated low density lipoproteins. Absence of contamination with smooth muscle cells >2% was verified by counterstaining of cell nuclei with bisbenzimide and with an antibody against smooth muscle α-actin. ECs were collected from a single Petri dish using gentle trypsinization beginning 10 ± 1 min before the start of incubation. The resulting cell suspension was subjected to gentle centrifugation at 200 × g, and cells were washed twice with Krebs-Henseleit buffer, resuspended in 5 ml of Krebs buffer containing 10% newborn calf serum, and kept at 37 °C in a culture tube. ECs were added to the incubation cuvette immediately before the start of the experiment, and the cell suspension was subjected to continuous low speed stirring using an electromagnetic cuvette-stirring unit.

Anesthetized male Wistar rats (300–350 g) were killed, and the thoracic aortas were carefully removed, cleaned up of fat and connective tissue, and cut into 4–5-mm rings. The endothelial integrity of these vascular rings was verified by their ability to relax, in an organ bath, on addition of 1 μM acetylcholine by ≥70% of the precontraction level achieved with phenylephrine. Vascular rings were kept in phosphate-buffered saline at 37 °C for up to 30 min before addition to the incubation cuvette. Vascular tissue was kept at the bottom of a 3-ml cuvette without stirring.

Computer Simulation—Simulations for development of a mathematical model to explain the observed results were run using Stella II (Version 1.02; High Performance Systems, Hanover, NH) on a Power Macintosh 7200/90 (Apple Computers) with numerical regression of the Runge-Kutta fourth derivative (24) (for the rate equations used, see "Results"). Calculated metHb and ferrocytochrome c concentrations were plotted as a function of time and converted into absorbance units using the molar extinction coefficients for the NO/oxyHb and O_2^-/ferricytochrome c reactions determined for the combined assay (see "Results").

Calculations and Statistics—The raw data output of the photodiode array spectrophotometer was transferred via the serial interface to a personal computer and stored in individual files for later processing by a commercial graphics and data analysis software (Origin 4.0; MicroCal Inc., Northampton, MA). Base-line smoothing was achieved by applying the method of moving average. With an increasing number of consecutive data points set in relation to one original data point, base-line noise decreases, and thus, sensitivity increases provided the length of the averaging interval does not exceed the length of the signal to be monitored (for the effect of this procedure on base-line noise, see Fig. 2). In contrast, assay sensitivity for fast kinetics is improved, and changes in peak shape are avoided by selecting rather short intervals. Usually, an averaging interval of 5–10 s was used for rapid kinetics and 30–240 s for slower reactions. This flexibility in choice of the most appropriate averaging interval adds to the general advantage of the diode array technique over conventional spectrophotometry, *i.e.* the possibility of adjusting the data processing with respect to the signal without loss of original data points after the actual measurement has taken place.

Results are presented as means ± S.D. The rates of formation in either assay system are reported as net values corrected for the blank determined under the same conditions, but in the absence of an NO- or O_2^--generating system. As pilot tests revealed that the presence of oxyHb causes slow, superoxide dismutase-independent reduction of ferricytochrome c over time, all measurements for direct comparison of the "classical" cytochrome c assay with the combined NO/O_2^- assay were performed in the presence of 5 μM oxyHb. Intra- and interassay comparisons were made applying the Mann-Whitney U test for unpaired variables, and a p value of <0.05 was accepted to denote statistical significance.

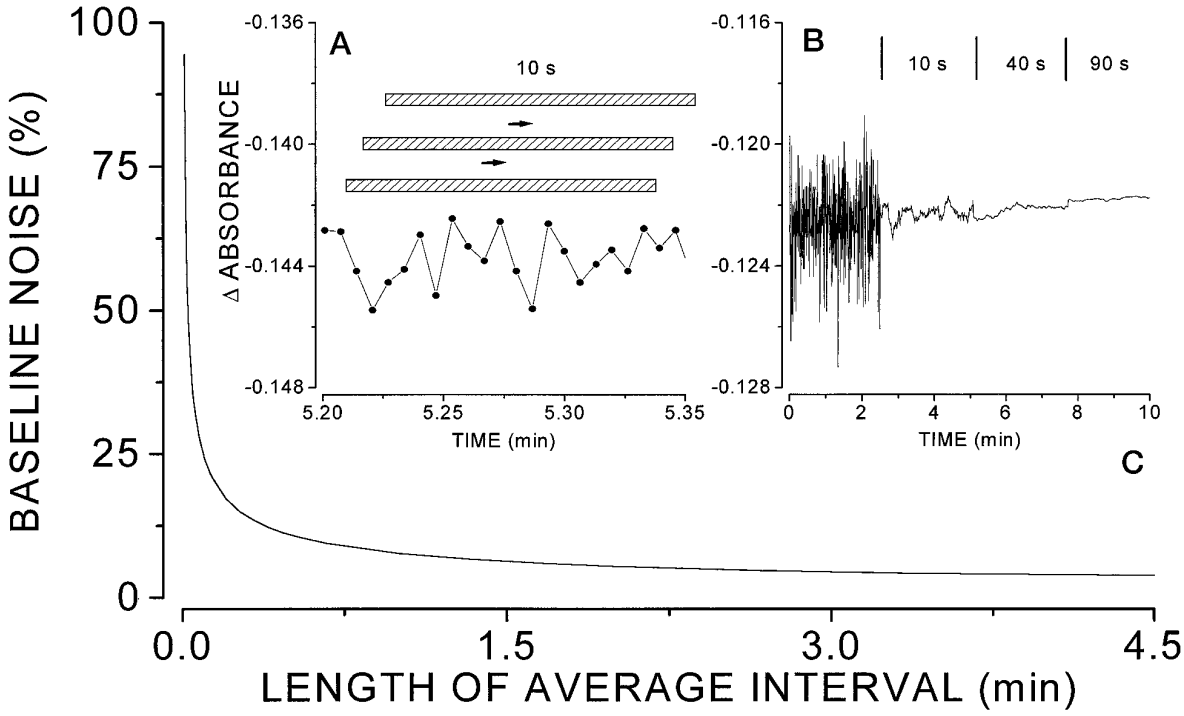

FIG. 2. **Principle of post-processing of photometric detector signals using the method of moving average.** *A*, photometric readings were obtained at a sampling rate of 2 Hz (*i.e.* every 0.5 s), and a given set of consecutive data points was used for calculation of mean values. The chosen averaging interval (here, 10 s) moves along the time axis (indicated here by *three hatched bars* of the same 10-s interval, with *arrows* indicating the direction of movement) during photometric measurement to continuously calculate mean values without loss of single data points. *B*, shown is the original photometric tracing demonstrating the decrease in base-line noise with increasing length of averaging interval. *C*, illustrated is the relationship between the signal noise and the length of the averaging interval.

RESULTS

Wavelength Selection and Optimal Concentration Ratio—To select the optimal wavelengths that would allow the simultaneous and independent monitoring of the redox conversion of either hemoprotein, spectral changes of the individual reactions were compared. The classical wavelengths of either assay (*i.e.* 401 and 411.5 nm for the oxyHb assay and 550 nm for the cytochrome *c* assay) could not be used for a combined assay as they overlap with opposite spectral changes of the respective other reaction (see difference spectra depicted in Fig. 1, *A* and *B*). However, an isosbestic point was found at 525 nm, a wavelength at which absorbance changes of either reaction were negligible. 541.2 nm, which represents an isosbestic point for the ferri- to ferrocytochrome *c* conversion, was chosen for recording of the changes in oxyHb concentration, and 465 nm, a point at which absorbance changes for the conversion of oxyHb to metHb are negligible, was chosen for monitoring the ferri- to ferrocytochrome *c* conversion (Fig. 3, *A–C*).

H_2O_2, which can be formed by the spontaneous or enzymatic (superoxide dismutase-mediated) dismutation of O_2^-, has the potential to interfere with either hemoprotein (25, 26), in particular at higher rates of O_2^- generation. Therefore, catalase was added, and a final concentration of 100 units/ml was found to be sufficient to completely prevent erroneous absorbance changes (false positive oxyHb oxidation and partial reversal of ferricytochrome *c* reduction) caused by this oxidant. Although a hemoprotein as well, catalase did not affect the absorbance spectrum of the ferricytochrome *c*/oxyHb mixture at this low concentration. Likewise, the measured rates of NO formation generated by 20 μM spermine NONOate were virtually identical in the absence and presence of this concentration of catalase using either the combined assay or the classical oxyHb technique (n = 2 each) (data not shown).

Initial experiments were carried out with equimolar concentrations of ferricytochrome *c* and oxyHb (5 μM each), which required slightly different detection wavelengths and molar extinction coefficients (data not shown). By systematic variation of the concentration ratio of either hemoprotein (5:5, 5:10, 5:15, and 5:20 and 10:5, 15:5, and 20:5 for ferricytochrome *c* and oxyHb, respectively; n = 2–3 for each concentration ratio) and the use of the hypoxanthine/xanthine oxidase system for generation of O_2^- and spermine NONOate for generation of NO, it was found that the trapping efficacy O_2^- approached an optimum at a ferricytochrome *c*/oxyHb molar ratio of 4:1. The recovery of NO at a ferricytochrome *c*/oxyHb ratio of 4:1 was not significantly different from that at a ratio of 1:1 as evidenced by comparison of the rates of NO generation from 20 μM spermine NONOate under both conditions (586.0 ± 12.5 *versus* 594.6 ± 38.1 nM NO/min at 4:1 and 1:1 ferricytochrome *c*/oxyHb, respectively, at 37 °C and pH 7.4; n = 5). However, O_2^- recovery increased by almost 50% at higher ferricytochrome *c* concentrations, both in the absence and presence of simultaneous NO generation (901.2 ± 136.6 *versus* 604.3 ± 93.7 nM O_2^-/min, respectively, with 25 μM hypoxanthine and 0.75 milliunit of xanthine oxidase at 37 °C and pH 7.4; $p < 0.05$, n = 5). There was no significant difference in measured O_2^- rates between 15 and 20 μM ferricytochrome *c*. Concentrations higher than 20 μM ferricytochrome *c* could not be tested in the presence of 5 μM oxyHb due to technical limitations (too high an absorbance for auto-zeroing of the diode array photometer). Final concentrations of 20 μM ferricytochrome *c* and 5 μM oxyHb were thus chosen for all further experiments. The molar extinction coefficients under these conditions were determined to be $\epsilon_{465-525}$ = 7.3 mM^{-1} cm^{-1} for the conversion of ferri- to ferrocytochrome *c* using ascorbate as reductant and $\epsilon_{541.2/525}$ = 6.6 mM^{-1} cm^{-1} for the oxyHb to metHb conversion using spermine NONOate as NO donor. Assay reproducibility was better than 4% (coefficient of variance = 3.7; n = 12).

Assay Validation—Selectivity of specific wavelengths for the measurement of NO and O_2^- was assessed as follows. Repeated

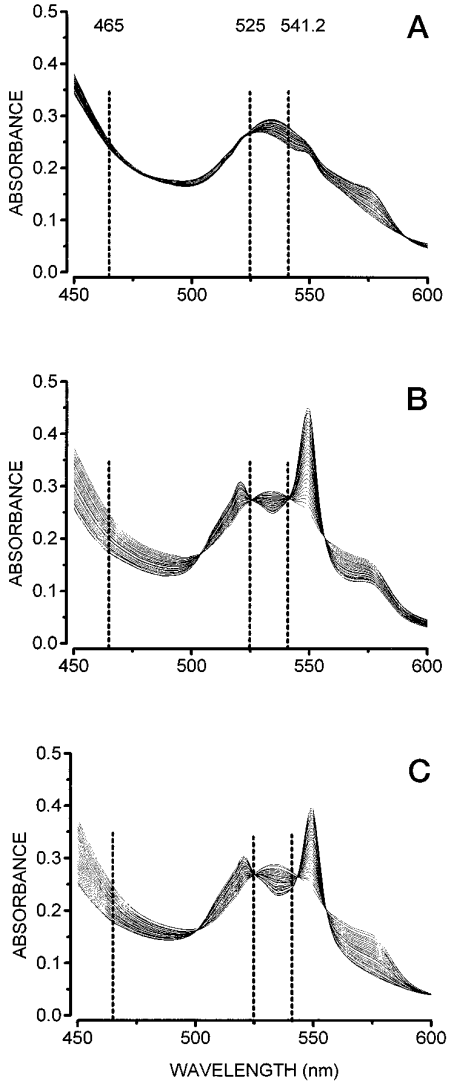

FIG. 3. **Repetitive difference spectral scans of a mixture of oxyHb and ferricytochrome *c*.** Scans were recorded at 20-s intervals in phosphate buffer, pH 7.4, supplemented with 5 μM oxyHb, 20 μM ferricytochrome *c*, and 100 units/ml catalase at 37 °C. *A*, conversion of oxyHb to metHb by NO released from spermine NONOate (20 μM); *B*, reduction of ferricytochrome *c* by O_2^- generated from hypoxanthine (25 μM)/xanthine oxidase (0.7 unit/liter); *C*, simultaneous conversion of oxyHb to metHb and ferri- to ferrocytochrome *c* by generation of NO and O_2^- as in *A* and *B*. *Dashed lines* indicate wavelengths chosen for monitoring absorbance changes of redox conversion of hemoglobin and cytochrome *c* in the nitric oxide/superoxide assay. *541.2* nm is the wavelength used for recording the absorbance difference for oxyHb to metHb conversion; *465* nm is the wavelength used for monitoring ferri- to ferrocytochrome *c* conversion; and *525* nm is the isosbestic point for the reduced and oxidized forms of either hemoprotein.

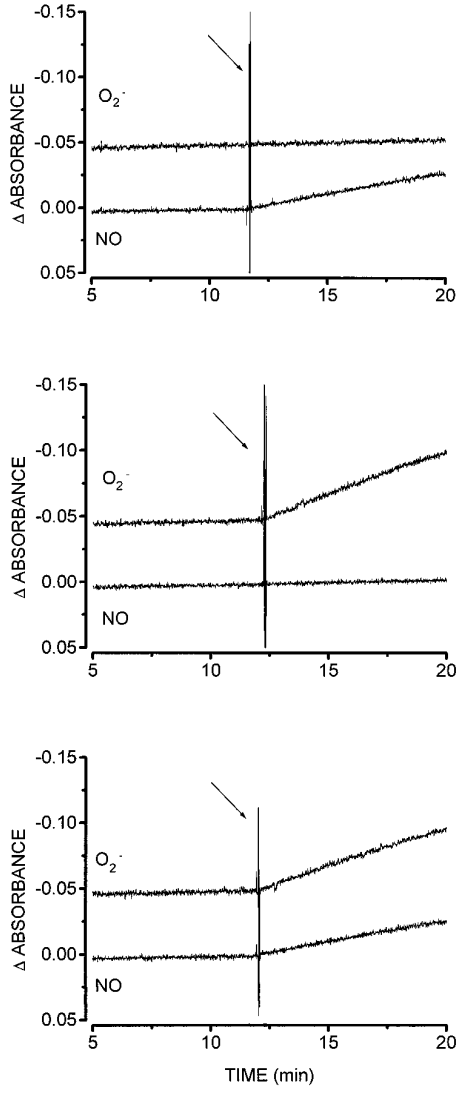

FIG. 4. **Original tracings demonstrating the specificity of the nitric oxide/superoxide assay.** Concentrations of hemoproteins, catalase, spermine NONOate, and hypoxanthine/xanthine oxidase were the same as those given in the legend to Fig. 3. *Upper panel*, the generation of NO from the NO donor spermine NONOate resulted in the time-dependent formation of NO without affecting the photometric signal for O_2^-. *Middle panel*, the generation of O_2^- by a mixture of hypoxanthine and xanthine oxidase selectively increased the rate of reduction of ferricytochrome *c* without affecting the photometric signal for NO. *Lower panel*, the simultaneous formation of NO and O_2^- resulted in the parallel increase in both photometric signals at rates indistinguishable from those of the individual reactions. The *arrows* indicate the time of addition of the NO- and O_2^--generating systems.

addition of aliquots of an aqueous solution of authentic NO (final concentration = 0.2–1 μM) to a mixture of oxyHb and ferricytochrome *c* in phosphate buffer, pH 7.4, produced stepwise increases in the absorbance difference between 541.2 and 525 nm, indicative of metHb formation, without inducing any changes in the absorbance difference between 465 and 525 nm, demonstrating that the cytochrome *c* signal was unaffected (n = 5) (data not shown). Likewise, selective gradual increases in metHb formation were seen when NO was continuously generated by the NO donor compound spermine NONOate (Fig. 4, *upper panel*). Measured rates of NO formation by spermine NONOate in the combined assay were identical, within experimental error, to those obtained with oxyHb alone (Table I), demonstrating that NO detection is not influenced by the presence of cytochrome *c*. Likewise, addition to the ferricytochrome *c*/oxyHb mixture of aliquots of a stock solution of KO_2 in dimethyl sulfoxide resulted in a stepwise reduction of ferricytochrome *c* without changes in the hemoglobin signal (n = 3) (data not shown). In the presence of the O_2^--generating hypoxanthine/xanthine oxidase system, a selective increase in the absorbance difference between 465 and 525 nm was observed (Fig. 4, *middle panel*). In the presence of the same concentration of both spermine NONOate and hypoxanthine/xanthine oxidase, *i.e.* under conditions of simultaneous generation of NO and O_2^-, measured individual rates of radical formation were identical to the separately determined rates (Fig. 4, *lower panel*). This indicates that the concentrations of oxyHb and ferricytochrome *c* present in the combined assay are sufficient to effectively trap all of the NO and O_2^- generated. As for NO, the measured rates of O_2^- formation using the combined assay were

TABLE I
Comparison of classical oxyhemoglobin and cytochrome c assays with the combined nitric oxide/superoxide assay

Nitric oxide was generated at either low (↓) or high (↑) rates from the NO donor spermine NONOate (4 and 40 μM); O_2^- was enzymatically generated at two different formation rates to approximately match the NO fluxes applied using xanthine oxidase/hypoxanthine (0.1 unit/liter and 10 μM, respectively, for the low (↓) and 0.75 unit/liter and 25 μM, respectively, for the high (↑) flux rates). The data presented are the mean ± S.D. of five individual incubations (initial rates were determined between 0.5 and 10 min after the start of the reaction).

Conditions	Classical assay systems	Combined NO/O_2^- assay	Level of significance
	μM/min	*μM/min*	
NO (↓)	0.085 ± 0.005	0.083 ± 0.008	NS[a]
NO (↑)	0.949 ± 0.013	0.941 ± 0.098	NS
O_2^- (↓)	0.128 ± 0.013	0.116 ± 0.016	NS
O_2^- (↑)	1.042 ± 0.047	0.974 ± 0.106	NS

[a] NS, not significant.

not significantly different from those determined with the classical cytochrome *c* assay (Table I). The slightly (<10%) smaller rates of O_2^- formation using the combined NO/O_2^- assay compared with the classical cytochrome *c* assay (Table I) may be explained by reaction of O_2^- with oxyHb, which, although comparatively slow (27), may partially compete with the trapping by ferricytochrome *c* under these conditions. Absorbance changes for the ferri- to ferrocytochrome *c* conversion elicited by high concentrations of hypoxanthine/xanthine oxidase (producing flux rates of ~1 μM O_2^-/min) were completely (>96%) abolished in the presence of 100 units/ml superoxide dismutase, confirming the specificity of the signal for O_2^-. In a separate set of experiments, the recovery of NO and O_2^- at low (0.1 μM/min) and high (1 μM/min) flux rates was additionally tested in a crossover design under conditions of simultaneous formation of both radicals at either equimolar generation rates or at a 10-fold excess of one radical over the other (Table II). Under all conditions, *i.e.* at equimolar flux rates as well as at 10-fold higher generation rates of NO over O_2^- and vice versa, individual rates of formation significantly differed neither from each other nor from the rates measured in the absence of the respective other radical (compare Tables I and II).

Maximal assay sensitivity suitable for monitoring relatively slow changes in cellular metabolic activity was calculated to approach 25 nM for NO and O_2^- production, respectively, using 240 s as the time interval for data post-processing, applying the method of moving average (see "Experimental Procedures" for details). Shorter averaging intervals (10–30 s), which are recommended for routine monitoring of rapid concentration changes, decrease the detection limit to ~100–60 nM for either radical (calculated for a signal-to-noise ratio of 3:1).

Reactions to $ONOO^-$—Because NO and O_2^- react at an almost diffusion-controlled rate to form $ONOO^-$ and because the oxyHb assay has been reported to cross-react with $ONOO^-$ (28), we sought to investigate what absorbance changes occur on addition of peroxynitrite to the combined NO/O_2^- assay. Consecutive addition to the ferricytochrome *c*/oxyHb mixture of authentic $ONOO^-$ resulted in stepwise contrary changes in the absorbance difference for each signal, indicating oxidation of both oxyHb and ferrocytochrome *c* (Fig. 5). Interestingly, the extent of oxidation was dependent on the concentration of $ONOO^-$ as well as on the concentration of oxyHb and ferrocytochrome *c*, with decreasing efficacy at lower hemoprotein concentrations. The quantum yield of this reaction as estimated from the sum of oxidized ferrocytochrome *c* and oxyHb in relation to the concentration of $ONOO^-$ applied was in the range of 3–10% at 100 and 10 μM $ONOO^-$, respectively (n = 3). Controls with solutions of decomposed $ONOO^-$ at identical pH were found to have no effect (n = 2), confirming that the observed changes in the absorbance difference were not the result of an artifactual change in pH. Moreover, the difference spectrum of the reaction of $ONOO^-$ with oxyHb was indistinguishable from that obtained with oxyHb and authentic NO, whereas that of ferrocytochrome *c* and $ONOO^-$ was the mirror image of that obtained with ferricytochrome *c* and O_2^-. Thus, whereas $ONOO^-$ appears to mimic NO in its reaction with oxyHb, it produces spectral changes opposite to those elicited by O_2^-. Methionine was found to inhibit the oxidation by $ONOO^-$ of ferrocytochrome *c* and oxyHb in a concentration-dependent manner (tested at 1–50 mM; maximal effects at 20 mM), presumably via oxidation of its thioether group to form the corresponding sulfoxide. Other known $ONOO^-$ scavengers such as ascorbate, cysteine, ebselen, and glutathione (all tested at 0.01–1 mM) could not be used in this assay because of redox interferences with one or the other hemoprotein.

TABLE II
Simultaneous quantification of NO and O_2^- formed at different rates using the nitric oxide/superoxide assay

NO and O_2^- were generated at two different flux rates. Sources of and conditions for NO and O_2^- generation were identical to those given in legend to Table I Neither the low (↓) nor the high (↑) formation rates of NO differed statistically from each other when measured in the presence of low and high flux rates of O_2^- and vice versa. Data are given as the means ± S.D. of five to seven individual kinetic runs determined at 3 different days.

Conditions	NO	O_2^-
	μM/min	*μM/min*
NO (↓)/O_2^- (↓)	0.081 ± 0.012	0.116 ± 0.017
NO (↓)/O_2^- (↑)	0.090 ± 0.013	0.915 ± 0.049
NO (↑)/O_2^- (↓)	0.940 ± 0.050	0.123 ± 0.046
NO (↑)/O_2^- (↑)	0.943 ± 0.050	0.971 ± 0.083

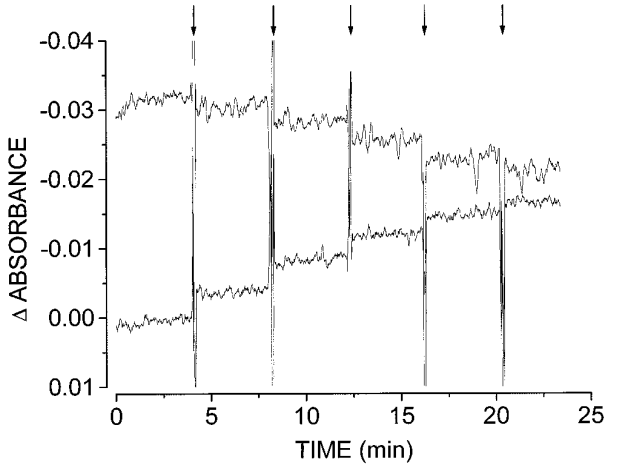

FIG. 5. **Original tracings demonstrating the effect of peroxynitrite on the photometric signals for redox conversion of hemoglobin and cytochrome *c*.** 10-μl aliquots of a stock solution of authentic $ONOO^-$ (final concentration = 10 μM) were repeatedly added (indicated by the *arrows*) to the cytochrome *c*/oxyHb assay mixture (20 and 5 μM, respectively) with continuous recording of absorbance differences at 541.2/525 and 465/525 nm. The *upper tracing* depicts the successive oxidation by $ONOO^-$ of the portion of reduced cytochrome *c* contained in the ferricytochrome *c*/oxyHb mixture. The *lower tracing* demonstrates the parallel oxidation by $ONOO^-$ of oxyHb to metHb.

In Vitro Applications—In addition to the validation experiments described before, a separate set of investigations was performed using SIN-1 as model compound for the simultaneous generation of NO and O_2^- (29). Addition of SIN-1 to the assay mixture resulted in a time-dependent increase in absorbance for both the NO and O_2^- signals (Fig. 6). Increases in ferrocytochrome *c* formation by SIN-1 were completely inhibited in the presence of 5 units/ml superoxide dismutase (n = 2). The release of NO and O_2^- from 100 μM SIN-1 at pH 7.40 and

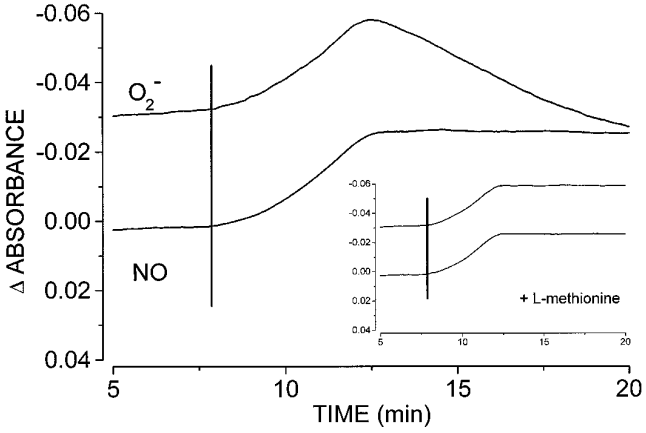

FIG. 6. **Representative tracings of parallel on-line measurement of the co-generation of NO and O_2^- during the nonenzymatic decay of SIN-1 (100 μM) using the nitric oxide/superoxide assay.** Experimental conditions were the same as described in the legend to Fig. 3. The *vertical bars* indicate the time of addition of SIN-1, which, after a short lag phase due the prior hydrolysis to SIN-1A (29), produces NO and O_2^- at rates of 1.24 and 1.12 μM/min, respectively. After all of the oxyHb is consumed, the ongoing generation of both radicals by excess SIN-1 leads to formation of $ONOO^-$, which in turn converts ferrocytochrome *c* back to ferricytochrome *c*, as indicated by the negative slope of the O_2^- signal. *Inset*, L-methionine (20 mM), added to the incubation buffer at time 0, effectively scavenges $ONOO^-$, thus preventing ferrocytochrome *c* oxidation without affecting the rates of formation of NO and O_2^-.

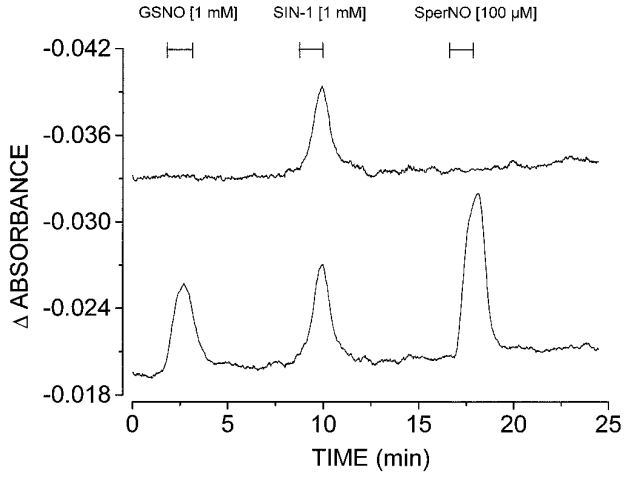

FIG. 7. **Original tracings of the nitric oxide/superoxide assay in the flow-through mode.** *Lower tracing*, absorbance changes of the conversion of oxyHb to metHb; *upper tracing*, absorbance changes of the conversion of ferri- to ferrocytochrome *c*. A chromatography column was perfused with Hepes (25 mM)-modified Krebs-Henseleit buffer, pH 7.40 (37 °C), supplemented with catalase (100 units/ml), oxyHb (5 μM), and ferricytochrome *c* (20 μM) at a flow rate of 2 ml/min. The column effluent was passed through a flow-through cuvette with continuous monitoring of absorbance changes at 465, 525, and 541.2 nm. Infusion (0.02 ml/min) of stock solutions of the NO donor compounds *S*-nitrosoglutathione (*GSNO*; 1 mM) and spermine NONOate (*SperNO*; 100 μM) into the perfusion line selectively induced absorbance changes in the hemoglobin signal corresponding to maximal NO concentrations of 1.02 and 2.06 μM, respectively. Infusion of SIN-1 (1 mM) produced absorbance changes in both channels, indicating simultaneous formation of NO and O_2^-. Maximal steady-state concentrations achieved with 1 mM SIN-1 under these conditions corresponded to 1.23 μM NO and 1.24 μM O_2^-.

37 °C was determined to be 1.24 ± 0.07 μM NO/min and 1.12 ± 0.04 μM O_2^-/min (n = 3), which is in good agreement with the proposed mechanism of oxidative breakdown of sydnonimines (30, 31). Interestingly, the increase in the cytochrome *c*-related signal turned into a decrease of about the same rate after all of the oxyHb was consumed by reaction with NO. This is explained by a reoxidation of the formed ferrocytochrome *c* by $ONOO^-$, which is produced when NO is no longer scavenged by oxyHb and was found to continue until all of the ferrocytochrome *c* was completely converted to ferricytochrome *c*. In agreement with this assumption, addition of fresh oxyHb to such incubations resulted in a reversal of this phenomenon, with further increases in both the NO and O_2^- signals until all of the oxyHb was consumed again (n = 2) (data not shown). Addition of 20 mM L-methionine completely prevented ferrocytochrome *c* reoxidation without affecting the initial rates of NO and O_2^- formation (Fig. 6, *inset*). These data suggest that, using this assay, measurements made in the presence and absence of methionine provide a straightforward means to additionally test for the presence of already formed $ONOO^-$. Identical results were obtained when NO and O_2^- were generated using spermine NONOate and hypoxanthine/xanthine oxidase (data not shown).

The on-line measurement of NO and O_2^- under conditions of continuous flow was demonstrated using a perfusion system with either phosphate buffer or Krebs-Henseleit buffer supplemented with 5 μM oxyHb and 20 μM ferricytochrome *c*, which was passed through a flow-through cell placed in the cuvette holder of the diode array spectrophotometer, and continuous recording of absorbance changes at 465, 525, and 541.2 nm. The flow rate of the system was adjusted to values of 1.0–10.0 ml/min by means of a low pulse peristaltic pump (Minipuls 3, Gilson Medical Electronics Inc., Middleton, WI), and calibration for NO and O_2^- was performed by coinfusion of small volumes (10–40 μl/min) of NO and KO_2 standards, respectively, using a high precision infusion pump (Precidor, Infors AG, Bottmingen, Switzerland). Provided dilution by the coinfusion of the total ferricytochrome *c*/oxyHb concentration in the buffer was kept below 0.5%, blanks with coinfused saline instead of NO or KO_2 did not produce any artifactual changes in absorbance. Linearity of the photometric response was demonstrated for NO concentrations in the range of 0.05–3 μM (r = 0.97; n = 15). Reproducibility was comparable to that for end point determinations (coefficient of variance = 5.6%; n = 24). Using this system, the flux rates of NO and O_2^- formation by three different classes of NO donor compounds (spermine NONOate, *S*-nitrosoglutathione, and SIN-1) were investigated (Fig. 7). Whereas the spontaneous decomposition in phosphate buffer of any one of the model compounds was found to be associated with the release of small amounts of NO, only in the case of SIN-1 was NO release accompanied by a stoichiometric generation of O_2^-.

Biological Applications—Having demonstrated the validity of the method for measuring NO and O_2^- in relatively simple *in vitro* systems, it was of interest to see whether or not it would be applicable to more complex biological systems without further modification. Two different biological sources were used to demonstrate, in a first pilot investigation, the suitability of the combined NO/O_2^- assay for application to intact cells and tissues: cultured aortic ECs and isolated vascular tissue. ECs in suspension were found to continuously release NO and O_2^- at low, yet detectable rates (n = 3) (Fig. 8*A*). NO was enhanced severalfold over basal release rates in the presence of the calcium ionophore A23187, whereas the signal for O_2^- was markedly suppressed (Fig. 8*B*). In contrast, addition of NADPH (data not shown) or NADH to ECs in suspension selectively increased the signal for O_2^-, leaving the NO signal virtually unaffected (Fig. 8*C*). In freshly isolated resting aortic tissue, the basal release of NO was below the quantifiable limit. Addition of NADH markedly increased the formation of O_2^- (Fig. 8*D*), and this increase was fully inhibitable by superoxide dismutase (n = 5) (Fig. 8*E*). These data clearly demonstrate that

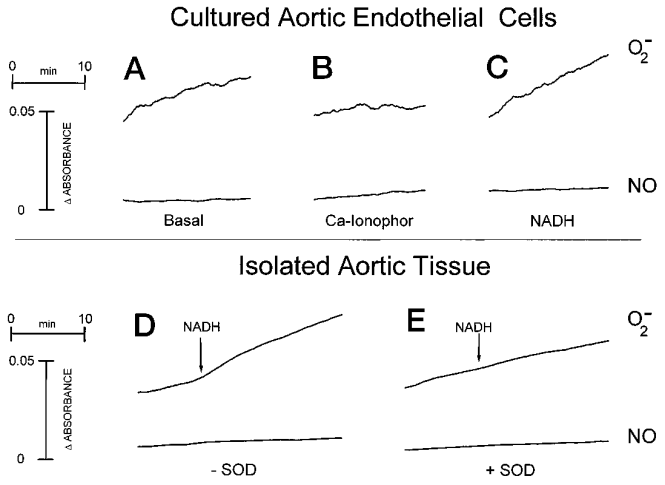

FIG. 8. **Basal and stimulated NO and O_2^- release in cultured aortic endothelial cells (*A–C*) and isolated aortic tissue (*D* and *E*).** *A*, basal release of NO and O_2^- from ECs with stirring; *B*, stimulation of NO formation and suppression of O_2^- release in the presence of the calcium ionophore A23187 (calcimycin, 500 nM); *C*, selective stimulation of O_2^- production by NADH (100 μM). The tracings depicted were obtained with the same batch of ECs (second passage). Recordings were started immediately after addition of ECs (corresponding to ~200 mg of protein) to an incubation solution containing 20 μM ferricytochrome *c*, 5 μM oxyHb, and 100 units/ml catalase in a total volume of 3 ml. In *B* and *C*, the incubation mixture was additionally supplemented with the appropriate stimulus prior to addition of the cells. Results are representative of three individual experiments performed in duplicate using two different batches of ECs. *D*, effect of addition of NADH (100 μM) on the production of NO and O_2^- from resting isolated aortic tissue in the absence of superoxide dismutase (*SOD*); *E*, complete inhibition by superoxide dismutase (100 units/ml) of the NADH-mediated increase in the ferricytochrome *c* signal. Recordings were started immediately after addition of aortic tissue (corresponding to ~2.5 mg of total protein) to an incubation mixture containing 20 μM ferricytochrome *c*, 5 μM oxyHb, and 100 units/ml catalase in a total volume of 3 ml. The *arrows* indicate the time of addition of NADH. The tracings depicted are representative of five experiments with identical results.

this method can also be used for reliable kinetic measurement of NO and O_2^- in biological samples.

Simulation Model—In our experiments, NO and O_2^- were formed simultaneously at specified rates. Under these conditions, either radical can undergo various reactions. To better understand the NO/O_2^- interaction, a theoretical model that allows the prediction of experimental results via a mathematical simulation was elaborated, which is based on the following assumptions and experimental evidence.

Superoxide can react with ferricytochrome *c* (Equation 6; $k_6 = 2 \times 10^6$ M^{-1} s^{-1}) (32), with NO to form $ONOO^-$ (Equation 1; $k_1 = 6 \times 10^9$ M^{-1} s^{-1}) (10), or dismutate spontaneously to give hydrogen peroxide (Equation 7; $k_7 = 5 \times 10^5$ M^{-1} s^{-1}) (33).

$$2\ O_2^- + 2H^+ \rightarrow H_2O_2 + O_2 \qquad \text{(Eq. 7)}$$

NO can react with oxyHb to form metHb (Equation 5; $k_5 = 3 \times 10^7$ M^{-1} s^{-1}) (34, 35) and with O_2^- as in Equation 1. Peroxynitrite can isomerize to yield nitrate (Equation 2) at a rate of $k_2 = 0.8$ s^{-1} (36). $ONOO^-$, presumably through the *s-trans*-isomer of ONOOH, which is a powerful oxidant. As seen in Figs. 6 and 9, addition of peroxynitrite does oxidize ferrocytochrome *c* to ferricytochrome *c*, suggesting that when oxyHb is consumed by NO, the resultant $ONOO^-$ formed upon protonation can either oxidize ferrocytochrome *c* or isomerize to form NO_3^-. This reaction rate is unknown; however, a value can be estimated based on our observations. We have shown that the reoxidation of ferrocytochrome *c* in the presence of fluxes of NO/O_2^- is abolished by methionine, indicating that $ONOO^-$ is the oxidant responsible for this reaction. In Fig. 9, after oxyhemoglobin is

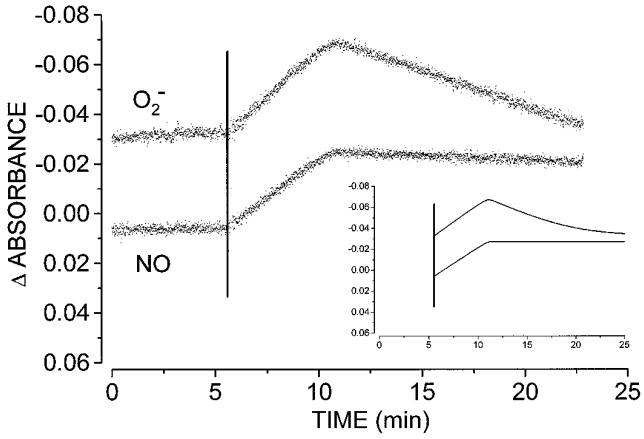

FIG. 9. **Comparison of computer simulation with experimentally obtained data.** NO and O_2^- were generated at equimolar flux rates of ~1 μM/min from spermine NONOate (40 μM) and a mixture of 0.75 unit/liter xanthine oxidase and 25 μM hypoxanthine in phosphate buffer, pH 7.4, at 37 °C. The *vertical bars* indicate the time of addition of NO- and O_2^--generating agents. The data points depicted were corrected for base-line drift. *Inset*, computer simulation of the absorbance changes for NO and O_2^- over time based on the measured flux rates of the actual experiment and the known rate constants for NO/O_2^- chemistry as described under "Results." Calculated concentrations were converted into absorbance units using the molar extinction coefficients determined experimentally. At any given time point, there is excellent agreement between simulated and experimentally obtained absorbance readings.

exhausted (300-s exposure to spermine NONOate and hypoxanthine/xanthine oxidase), the rate of reoxidation of ferrocytochrome *c* is ~50% that of the oxidation of oxyHb and the reduction of ferrocytochrome *c* in the previous 300 s. Although it is predicted that 100% of this flux would result in the formation of $ONOO^-$, this indicates that <50% actually oxidizes ferrocytochrome *c*, suggesting the involvement of competing reactions such as the rearrangement of protonated $ONOO^-$ to NO_3^- at a rate of 0.8 s^{-1} at neutral pH (Equation 2). Since ~50% of the ferrocytochrome *c* is oxidized by NO/O_2^-, we can approximate a rate constant for Equation 8,

$$\text{Ferrocytochrome } c \xrightarrow{ONOO^-} \text{ferricytochrome } c \qquad \text{(Eq. 8)}$$

by the following equation: 0.8 s^{-1}/5 $\times$ 10^{-6} M = 1.6 $\times$ 10^5 M^{-1} s^{-1} = k_8. Although it is unclear at this point whether $ONOO^-$ or ONOOH is the actual oxidant, this value is not out of line with $ONOO^-$ interaction with other metallocomplexes. It has been reported that hemoproteins such as myeloperoxidase react with $ONOO^-$ with a rate constant of 5 $\times$ 10^5 M^{-1} s^{-1} (37) and with Fe^{2+}-EDTA with a rate constant of 5700 M^{-1} s^{-1} (38), implying that such a rate constant for ferrocytochrome *c* is not unexpected.

The simulation was thus performed using the following rate equations: d[metHb]/dt = k_5[oxyHb][NO] (where $k_5 = 3 \times 10^7$ M^{-1} s^{-1}), d[ferrocytochrome *c*]/dt = k_6[ferricytochrome *c*][O_2^-] − k_8[$ONOO^-$][ferrocytochrome *c*] (where k_8= 1.6 $\times$ 10^5 M^{-1} s^{-1}), d[NO]/dt = k_{NO} − k_5[oxyHb][NO] − k_1[O_2^-][NO] (where k_{NO} = rate of NO generation), d[O_2^-]/dt = k_{sup} − k_6[ferricytochrome *c*][O_2^-] − k_1[O_2^-][NO] − k_7[O_2^-]^2 (where k_{sup} = rate of O_2^- generation), d[$ONOO^-$]/dt = k_1[O_2^-][NO] − k_8[$ONOO^-$][ferricytochrome *c*] − k_2[$ONOO^-$], d[NO_3^-] = k_2[$ONOO^-$], and d[H_2O_2]/dt = k_7[O_2^-]^2.

As depicted in Fig. 9, the simulated data are in good agreement with the data obtained experimentally. The most striking result from these simulations is the finding that $ONOO^-$ is not formed to any appreciable extent until >90% of the oxyHb is consumed. In addition to the high efficiency of oxyHb in trap-

ping NO, ferricytochrome *c* plays a significant role in maintaining low O_2^- levels. When the steady-state concentrations of NO and O_2^- were calculated at flux rates of ~1 μM/min for either radical in the presence of 5 μM oxyHb and 20 μM ferricytochrome *c*, these concentrations were maintained at <1 nM for NO and <10 nM for O_2^-. These data suggest that there is very little $ONOO^-$ formation in the presence of micromolar amounts of both hemoproteins. However, when oxyHb was exhausted, there was significant $ONOO^-$ formation as the levels of NO rose to ~80 nM, which is sufficiently high for O_2^- to be scavenged by NO instead of ferricytochrome *c*.

Two other conditions that are important for understanding the chemical reactions presented here, *i.e.* the simultaneous generation of NO and O_2^- in the absence of either oxyHb or ferricytochrome *c*, were simulated using our computer model. As seen from the experimental data, ferrocytochrome *c* is rapidly oxidized after oxyHb is consumed. Presumably, it is $ONOO^-$ that is responsible for this reaction as ferrocytochrome *c* is not readily oxidized by either NO or O_2^- under these conditions. When no oxyHb is present, ferrocytochrome *c* concentrations never rise above 10 nM as determined by simulation (assuming equimolar flux rates of 1 μM/min for NO and O_2^-, respectively). This is consistent with the observation that after oxyHb was exhausted, oxidation of ferrocytochrome *c* continued until it was completely converted into ferricytochrome *c*. How can $ONOO^-$ formation be so dominant under these conditions (no oxyHb), while in the absence of ferricytochrome *c*, oxyHb is readily oxidized with little contribution from $ONOO^-$? In the absence of ferricytochrome *c*, the O_2^- concentration rises to ~40 nM and slowly decays, which appears to be due to the dismutation kinetics (Equation 7) and reaction with NO (Equation 1) as the oxyHb concentration decreases. Under these conditions, NO is limiting; and hence, the factors that determine the kinetics are k_5[oxyHb] and $k_1[O_2^-]$. Since O_2^- never rises much above 45 nM (note: in the absence of either ferricytochrome *c* or oxyHb, the steady-state level is ~30 nM), the NO reaction with oxyHb will dominate. Conversely, in the sole presence of ferricytochrome *c* (0 μM oxyHb), NO continues to rise to levels of ~80–100 nM, where the NO/O_2^- reaction becomes significant (note: under these conditions, O_2^- concentrations do not rise above 1 nM). Since ferricytochrome *c* consumes O_2^-, NO levels would be expected to rise gradually until levels are reached where NO can compete for O_2^-. Since the concentration of ferrocytochrome *c* in the assay is only 20 μM, with a second-order rate constant for O_2^- of $2 \times 10^6\ M^{-1}\ s^{-1}$, it is not unexpected that significant $ONOO^-$ formation will occur at NO concentrations above 10 nM. These two different conditions clearly demonstrate the importance of oxyHb in preventing the formation of the deleterious molecule, $ONOO^-$. As the reaction between NO and O_2^- is near the diffusion-controlled limit, the importance of the role of hemoglobin in controlling the formation of $ONOO^-$ is often overlooked.

DISCUSSION

The most important finding of this study is that it is technically feasible to simultaneously monitor NO and O_2^- formation. The new nitric oxide/superoxide assay, for the first time, allows parallel, specific, and sensitive quantification of NO and O_2^- under conditions of simultaneous generation, although the chemical reaction between these radicals proceeds at an almost diffusion-controlled rate. Experimental data obtained with this assay were successfully simulated by a mathematical model that may provide a better understanding of the reaction of either radical with biomolecules such as hemoproteins. Moreover, the results obtained with cultured endothelial cells and isolated vascular tissue unambiguously demonstrate that this assay methodology is applicable to biological systems, too. Taken together, these new analytical tools may help to gain new insights into the physiological and pathophysiological significance of co-generated NO and O_2^- for maintenance and disturbance of cellular homeostasis.

The most striking feature of this new assay is that the chosen concentrations of hemoproteins are sufficient to almost completely trap all of the NO and O_2^- generated at any flux rate tested, thus allowing reliable quantification of either radical. Furthermore, this assay not only allows the quantification of the formation of NO or O_2^-, but also the study of their interaction. When one of the two hemoproteins is consumed entirely, *e.g.* when either all of the oxyHb is oxidized to metHb or all of the ferricytochrome *c* is reduced to ferrocytochrome *c*, NO and O_2^- react at an almost diffusion-controlled rate to form $ONOO^-$. More rapid than the isomerization of $ONOO^-$ to NO_3^- is its reaction with oxyHb or ferrocytochrome *c* (see Figs. 6 and 9). This, in addition, offers the possibility of using this assay for competitive kinetic studies. Addition of methionine, for example, an effective $ONOO^-$ scavenger, to the assay mixture of oxyHb and ferricytochrome *c* can unmask the presence of already formed $ONOO^-$. Thus, differences in the measured rates of formation of metHb or ferrocytochrome *c* in the absence and presence of methionine can be taken as indirect evidence for the involvement of $ONOO^-$.

Recently, it has been claimed that readings obtained with the classical oxyhemoglobin assay may not exactly reflect the amount of NO formed due to cross-reactivity of the assay with $ONOO^-$ (28). This interpretation is potentially misleading and requires re-evaluation in light of the findings of the present study. It is true that $ONOO^-$ can oxidize oxyHb (see Fig. 5), and the spectral changes observed are indistinguishable from those elicited by NO. Nevertheless, the absolute amount of NO formed (*i.e.* before its conversion to $ONOO^-$, NO_2^-, or NO_3^-, the ratio of which depends on the incubation conditions (7)) is correctly reflected even by the classical oxyHb assay as, contrary to other NO assay techniques, the photometric signal always represents the sum of both NO and $ONOO^-$. The nitric oxide/superoxide assay broadens analytical perspectives as it not only detects NO and simultaneously quantifies O_2^-, which probably accounts for most of its inactivation, but also allows the differentiation between conditions under which NO may or may not have already reacted with O_2^- to form $ONOO^-$. In contrast, in biological systems, Clarke-type electrodes (28), gas-phase chemiluminescence (21), and porphyrinic microsensors (39) allow only the quantification of the portion of NO that escapes reaction with O_2^-, molecular oxygen, and hemoproteins. Moreover, in contrast to the classical cytochrome *c* assay (40) and probably other assay systems for O_2^- as well, the nitric oxide/superoxide assay allows the correct quantification of the rate of O_2^- formation even in the presence of concomitantly generated NO. In summary, compared with classical analytical methods for separate measurement of either NO or O_2^-, this new assay offers specific, reliable, and simultaneous quantification of both radicals.

The use of the photodiode array technique for analysis of spectral changes associated with the redox conversion of hemoproteins offers several advantages over conventional photometric techniques. 1) A number of discrete wavelengths can be continuously monitored in parallel; 2) the post-processing of photometric signals permits reanalysis of spectral changes without the need for repetition of experiments originally run at suboptimal speed or sensitivity; 3) the assay is easy to handle, and the technical equipment required is much cheaper than that needed for conventional dual-wavelength double-beam spectrophotometry; and 4) the ability to perform full spectral scans at any time during the measurement provides a powerful

tool for on-line control of the specificity of the observed absorbance changes. Post-processing of raw data using the method of moving average resulted in a remarkably high sensitivity for NO and O_2^-. The detection limit for both radicals is below the physiologically relevant concentration range that we (41–43) and others (44, 45) previously determined in, for example, cultured endothelial cells and intact vascular tissue. Furthermore, the ratio of formation of either radical may vary considerably within one cell type depending on its activation status, as, for example, in macrophages immunologically challenged with cytokines (46). The nature of a given physiological, pharmacological, or immunological stimulus as well as the time between cellular exposure and analytical investigation will influence the ratio of NO, O_2^-, and $ONOO^-$ formed by these cells and may explain, at least in part, some of the discrepancy that can be found in the literature regarding experimental results. Under all these conditions, the nitric oxide/superoxide assay may help to resolve controversial issues. Besides future biological applications, this assay is also suitable for investigating NO and O_2^- formation by experimental drugs such as sydnonimines (see Fig. 6), for clarifying the mode of bioactivation of other NO donors in different tissues and cells, and for investigating the biochemical basis of certain endogenous counterregulatory mechanisms, which are, for example, associated with nitrate tolerance (47, 48).

The flexibility in choice of the most appropriate averaging interval constitutes an important advantage of this assay over conventional photometric techniques. Data can be easily reanalyzed with extended or shorter averaging intervals to achieve either greater sensitivity or better resolution for reactions with unexpectedly fast kinetics without loss of original data points. This will be of particular interest for analysis of radical formation in biological systems. Furthermore, the assay can be used at comparable sensitivity for end point determinations and continuous on-line measurement. Continuous quantification of NO and O_2^- represents an attractive analytical approach for investigation of reactive oxygen and nitrogen oxide formation in isolated organs under physiological and pathophysiological conditions.

The computer model developed from know rate constants allows the simulation of the reaction of both radicals with oxyHb and ferricytochrome *c*. From these results, insight is gained into the important role of redox-active proteins. These hemoproteins are abundantly present within and in close proximity to cells of the vascular wall and blood cells. Thus, because of the rapid reactions of NO and O_2^- with either hemoprotein, it is intriguing to speculate that hemoglobin and cytochrome *c* as well as other redox compounds may critically control both the reaction products and the degradation of NO and O_2^- *in vivo* and, by this, their biological effects. Since the reaction between NO and O_2^- is nearly diffusion-controlled, the importance of these hemoproteins can hardly be over-stressed, as the presence of micromolar concentrations already completely prevents formation of the potentially harmful species, $ONOO^-$. As revealed by computer simulation, equimolar flux rates of NO and O_2^-, when co-generated in the presence of ferricytochrome *c* and oxyHb, prevented formation of significant levels of $ONOO^-$ (and should thus prevent formation of other reactive nitrogen oxide species), as the steady-state concentration of NO is maintained at a low level by oxyHb. Besides thiols and tyrosine residues in proteins, the vicinity of oxyHb may be an additional limiting factor for $ONOO^-$ action in biological systems. Which factor(s) may, however, govern the extent of formation of $ONOO^-$ *in vivo* awaits further elucidation. Although data from our computer simulation suggest that, in the presence of certain hemoproteins, O_2^- may be the limiting factor, this may not be the case under other conditions. To shed light on these questions, one would need to know what the prevailing local concentrations of O_2^- are inside a cell in the vicinity of NO formation. Such data are not available yet.

The ability to simultaneously measure NO and O_2^- at physiologically relevant levels may be of particular interest for atherosclerosis research. Indirect evidence from recent studies using animal and human tissues suggest that the antiatherogenic and vasodilatory properties of NO are counteracted by an increased oxidative stress within the vascular wall (for review, see Ref. 8). Endothelial and vascular smooth muscle cells as well as monocytes, macrophages, and neutrophils are capable of producing both NO and O_2^- (for review, see Refs. 1, 3, 49, and 50). An imbalance in the formation of these radicals may have deleterious effects on vascular homeostasis. So far, this hypothesis is, however, supported by indirect evidence only (for review, see Refs. 50–52). In arterial hypertension, it has been speculated that endogenous NO production is compensatorily enhanced to counteract an increased oxidative stress within the vascular wall (9, 53, 54). Similarly, an imbalance in these radicals may be involved in the vascular dysfunction observed in diabetes mellitus and hyperlipoproteinemia (44, 55) and in the manifestation of functional disturbances following reperfusion of ischemic tissue and in myocardial ischemia and reperfusion injury, which has been shown to be associated with an increased formation of both oxygen free radicals (56) and NO (57) within the first minutes of reperfusion. The new assay, with its ability to simultaneously quantify both radicals in biological tissue, provides us with a powerful tool to experimentally challenge this yet hypothetical concept and to investigate the functional relevance of a shift in NO/O_2^- balance, providing a basis for the development of new therapeutic strategies for vascular protection.

Acknowledgments—We thank G. Alt, K. Knüttel, and R. Spahr for skillful technical assistance.

REFERENCES

1. Moncada, S., and Higgs, A. (1993) *N. Engl. J. Med.* **329,** 2002–2012
2. Snyder, S. H., and Bredt, D. S. (1992) *Sci. Am.* **266,** 68–77
3. Nathan, C., and Xie, Q. (1994) *Cell* **78,** 915–918
4. Lancaster, J. R., Jr. (1994) *Proc. Natl. Acad. Sci. U. S. A.* **91,** 8137–8141
5. Malinski, T., and Taha, Z. (1992) *Nature* **358,** 676–678
6. Bonner, F. T., and Stedman, G. (1996) in *Methods in Nitric Oxide Research* (Feelisch, M., and Stamler, J., eds) pp. 3–18, John Wiley & Sons Ltd., Chichester, England
7. Kelm, M., and Yoshida, K. (1996) in *Methods in Nitric Oxide Research* (Feelisch, M., and Stamler, J., eds) pp. 47–58, John Wiley & Sons Ltd., Chichester, England
8. Alexander, R. W. (1995) *Hypertension* (*Dallas*) **25,** 155–161
9. Kelm, M., Feelisch, M., Krebber, T., Deussen, A., Motz, W., and Strauer, B. E. (1995) *Hypertension* (*Dallas*) **25,** 186–193
10. Huie, R. E., and Padmaja, S. (1993) *Free Radical Res. Commun.* **18,** 195–199
11. Pryor, W. A., and Squadrito, G. L. (1995) *Am. J. Physiol.* **268,** L699–L722
12. Beckman, J. S., Wink, D. A., and Crow, J. P. (1996) in *Methods in Nitric Oxide Research* (Feelisch, M., and Stamler, J., eds) pp. 61–70, John Wiley & Sons Ltd., Chichester, England
13. Miles, A. M., Bohle, D. S., Glassbrenner, P. A., Hansert, B., Wink, D. A., and Grisham, M. B. (1996) *J. Biol. Chem.* **271,** 40–47
14. Feelisch, M., and Stamler, J. S. (eds) (1996) *Methods in Nitric Oxide Research*, John Wiley & Sons Ltd., Chichester, England
15. Abelson, J. N., and Simon, M. I. (1995) in *Methods: A Companion to Methods in Enzymology* (Everse, J., and Grisham, M. B., eds) Academic Press, New York
16. Greenwald, R. A. (ed) (1985) *CRC Handbook of Methods for Oxygen Radical Research*, CRC Press, Inc., Boca Raton, FL
17. van Assendelft, O. (ed) (1970) *Spectrophotometry of Hemoglobin Derivatives*, Charles C. Thomas Publisher, Springfield, IL.
18. Fridovich, I. (1985) in *CRC Handbook of Methods for Oxygen Radical Research* (Greenwald, R., ed) pp. 121–122, CRC Press, Inc., Boca Raton, FL
19. Hart, T. W. (1985) *Tetrahedron Lett.* **26,** 2013–2016
20. Feelisch, M. (1991) *J. Cardiovasc. Pharmacol.* **17,** S25–S33
21. Hampl, V., Walters, C. L., and Archer, S. L. (1996) in *Methods in Nitric Oxide Research* (Feelisch, M., and Stamler, J. S., eds) pp. 309–318, John Wiley & Sons Ltd., Chichester, England
22. Valentine, J. S., and Curtis, A. B. (1975) *J. Am. Chem. Soc.* **97,** 224–226
23. Pryor, W. A., Cueto, R., Jin, X., Koppenol, W. H., Ngu-Schwemlein, M., Squadrito, G. L., Uppu, P. L., and Uppu, R. M. (1995) *Free Radical Biol. & Med.* **18,** 75–83

24. Braun, M. (1975) *Differential Equations and Their Applications: An Introduction to Applied Mathematics,* pp. 159–163, Springer-Verlag New York Inc., New York
25. Vanderwalle, P. L., and Peterson, N. O. (1987) *FEBS Lett.* **210,** 195–198
26. Lemberg, R. (1956) *Rev. Pure Appl. Chem.* **6,** 1–23
27. Sutton, H. C., Roberts, P. B., and Winterbourn, C. C. (1976) *Biochem. J.* **155,** 503–510
28. Schmidt, K., Klatt, P., and Mayer, B. (1995) *Biochem. J.* **301,** 645–647
29. Feelisch, M., Ostrowski, J., and Noack, E. (1989) *J. Cardiovasc. Pharmacol.* **14,** S13–S22
30. Bohn, H., and Schönafinger, K. (1989) *Cardiovasc. Res.* **14,** 6–12
31. Feelisch, M., and Stamler, J. S. (1996) in *Methods in Nitric Oxide Research*, pp. 71–115, John Wiley & Sons Ltd., Chichester, England
32. Butler, J., Koppenol, W. H., and Margoliash, E. (1982) *J. Biol. Chem.* **257,** 10747–10750
33. Behar, D., Czapski, G., Rabani, J., Dorfman, and Schwarz, H. A. (1970) *J. Phys. Chem.* **74,** 3209–3213
34. Doyle, M. P., and Hoekstra, J. W. (1981) *J. Inorg. Biochem.* **14,** 351–358
35. Eich, R. F., Li, T., Lemon, D. D., Doherty, D. H., Curry, S. R., Aitken, J. F., Mathews, A. J., Johnson, K. A., Smith, R. D., Phillips, G. N., and Olson, J. O. (1996) *Biochemistry* **35,** 6976–6983
36. Beckman, J. S., Beckman, T. W., Chen, J., Marshall, P. A., and Freeman, B. A. (1990) *Proc. Natl. Acad. Sci. U. S. A.* **87,** 1620–1624
37. Floris, R., Piersma, S. R., Yang, G., Jones, P., and Wever, R. (1993) *Eur. J. Biochem.* **215,** 767–775
38. Beckman, J. S., Ischiropoulos, H., Zhu, L., van der Woerd, M., Smith, C., Chen, J., Harrison, J., Martin, J. C., and Tsai, M. (1992) *Arch. Biochem. Biophys.* **298,** 438–445
39. Malinski, T., Taha, Z., Grunfeld, S., Patton, S., Kapturczak, M., and Tomboulian, P. (1993) *Biochem. Biophys. Res. Commun.* **193,** 1076–1082
40. Thompson, L., Trujillo, M., Telleri, R., and Radi, R. (1995) *Arch. Biochem. Biophys.* **319,** 491–497
41. Kelm, M., Feelisch, M., Spahr, R., Piper, H.-M., Noack, E., and Schrader, J. (1988) *Biochem. Biophys. Res. Commun.* **154,** 236–244
42. Feelisch, M., Brands, F., and Kelm, M. (1995) *Eur. J. Clin. Invest.* **25,** 737–745
43. Kelm, M., and Schrader, J. (1990) *Circ. Res.* **66,** 1561–1575
44. Ohara, Y., Peterson, T. E., and Harrison, D. G. (1993) *J. Clin. Invest.* **91,** 2546–2551
45. Archer, S. (1993) *FASEB J.* **7,** 349–360
46. Denis, M. (1994) *J. Leukocyte Biol.* **55,** 682–684
47. Harrison, D. G., and Bates, J. N. (1993) *Circulation* **87,** 1461–1467
48. Münzel, T., Sayegh, H., Freeman, B. A., Tarpey, M. M., and Harrison, D. G. (1995) *J. Clin. Invest.* **95,** 187–194
49. Knowles, R. G., and Moncada, S. (1994) *Biochem. J.* **298,** 249–258
50. Katusic, Z. S. (1996) *Free Radical Biol. Med.* **20,** 443–448
51. Flavahan, N. A. (1992) *Circulation* **85,** 1927–1938
52. Griendling, K., and Alexander, R. W. (1996) *FASEB J.* **10,** 283–292
53. Nava, E., Noll, G., and Lüscher, T. F. (1995) *Circulation* **91,** 2310–2313
54. Nakazono, K., Watanabe, N., Matsuno, K., Sasaki, J., Sato, T., and Inoue, M. (1991) *Proc. Natl. Acad. Sci. U. S. A.* **88,** 10045–10048
55. Stehouwer, C. D. A., and Schaper, N. C. (1996) *Eur. J. Clin. Invest.* **26,** 535–543
56. Garlick, P. B., Davies, M. J., Hearse, D. J., and Slater, T. F. (1987) *Circ. Res.* **61,** 757–760
57. Zweier, J. L., Wang, P., and Kuppusamy, P. (1995) *J. Biol. Chem.* **270,** 304–307